

1 **A process-conditioned and spatially consistent method for reducing**
2 **systematic biases in modeled streamflow**

3
4 Andrew Bennett,^{a,b} Adi Stein,^a Yifan Cheng,^c Bart Nijssen,^a Marketa McGuire,^d

5 ^a *Department of Civil & Environmental Engineering University of Washington, Seattle, WA*

6 ^b *Department of Hydrology and Atmospheric Sciences, University of Arizona, Tucson, AZ*

7 ^c *National Center for Atmospheric Research, Boulder, CO*

8 ^d *Technical Service Center, US Bureau of Reclamation, Denver, CO*

9
10 *Corresponding author: Bart Nijssen, nijssen@uw.edu*

11

ABSTRACT

Water resources planning often uses streamflow predictions made by hydrologic models. These simulated predictions have systematic errors which limit their usefulness as input to water management models. To account for these errors, streamflow predictions are bias-corrected through statistical methods which adjust model predictions based on comparisons to reference datasets (such as observed streamflow). Existing bias-correction methods have several shortcomings when used to correct spatially-distributed streamflow predictions. First, existing bias-correction methods destroy the spatio-temporal consistency of the streamflow predictions, when these methods are applied independently at multiple sites across a river network. Second, bias-correction techniques are usually built on time-invariant mappings between reference and simulated streamflow without accounting for the processes which underpin the systematic errors.

We describe improved bias-correction techniques which account for the river network topology and allow for corrections that account for other processes. Further, we present a workflow that allows the user to select whether to apply these techniques separately or in conjunction. We evaluate four different bias-correction methods implemented with our workflow in the Yakima River Basin in the Northwestern United States. We find that all four methods reduce systematic bias in the simulated streamflow. The spatially-consistent bias-correction methods produce spatially-distributed streamflow as well as bias-corrected incremental streamflow, which is suitable for input to water management models. We demonstrate how the spatially-consistent method avoids creating flows that are inconsistent between upstream and downstream locations, while performing similar to existing methods. We also find that conditioning on daily minimum temperature, which we use as a proxy for snowmelt processes, improves the timing of the corrected streamflow.

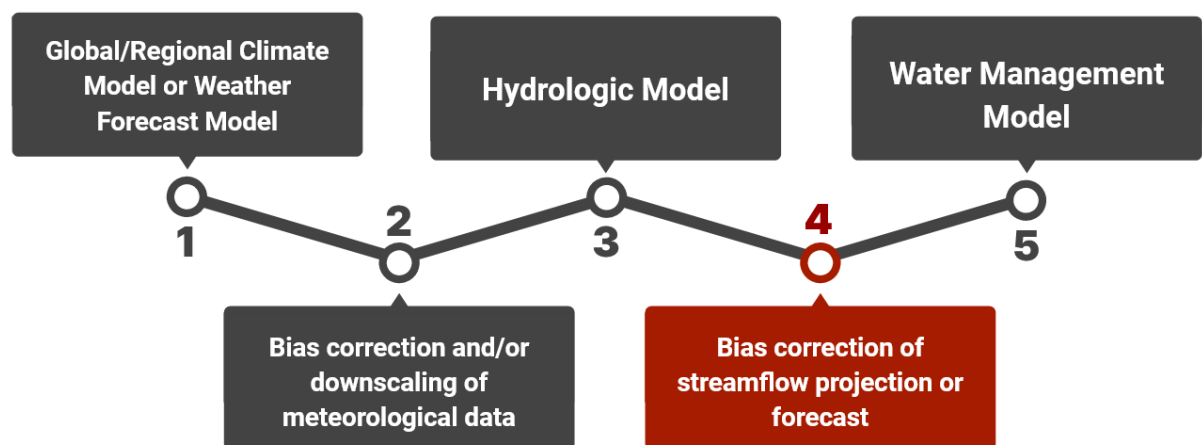
SIGNIFICANCE STATEMENT

To make streamflow predictions from hydrologic models more informative and useful for water resources management they are often post-processed by a statistical procedure known as bias-correction. In this work we develop and demonstrate bias-correction techniques which are specifically tailored to streamflow prediction. These new techniques will make modeled streamflow predictions more useful in complex river systems undergoing climate change.

1. Introduction

43 The use of computational models of hydrologic systems has become a nearly ubiquitous
 44 way to forecast streamflow and plan for the allocation of water resources. However, these
 45 predictions are often biased, because they are subject to systematic errors in the model inputs,
 46 model parameter values, and process representations. Regardless of the source of these errors,
 47 which are often difficult to determine, the introduction of such biases in predictions degrades
 48 their quality. To address these biases, it is common to “bias-correct” or “post-process” these
 49 predictions through some statistical procedure (Chen et al. 2013; Guo et al. 2020; Hashino et
 50 al. 2007). These corrections are particularly important when simulated streamflow values are
 51 used as input to water resources models, in which specific streamflow and storage thresholds
 52 trigger water management decisions. We refer to these correction methods generally as “bias-
 53 correction” techniques for simplicity, though they typically correct for the entire range of
 54 distributional errors rather than only for an overall bias in the mean.

55 Bias-corrections are commonly applied at multiple steps and to multiple variables along
 56 the modeling chain (e.g. those described by Bosshard et al. 2013 and Wilby and Dessai
 57 2010), most often precipitation and temperature in atmospheric model output and streamflow
 58 in hydrologic model output. While these modeling chains are not all exactly alike, they do
 59 contain some commonalities that are relevant to this study (Figure 1). Depending on the
 60 spatial and/or temporal scale considerations a climate model (either a finer-scaled regional
 61 model or a coarser-scale global model) or a weather forecast model is used to generate
 62 meteorologic forcing data. This forcing data is often bias-corrected and possibly downscaled
 63 to a finer spatiotemporal resolution to drive the hydrologic model. Following running a
 64 hydrologic model the predicted streamflow is also commonly bias-corrected before being
 65 used in a water management model to make management decisions.



66
 67 Figure 1. An example of the type of hydrologic modeling chain that we considered when
 68 developing our streamflow bias correction methods (step 4, highlighted in red).

70 Most studies in the bias-correction literature deal with the correction of atmospheric
71 variables (corresponding to step 2 in figure 1), especially in the context of climate change
72 studies (Cannon 2018; Maraun 2013; Pierce et al. 2015; Shi et al. 2008; Wood et al. 2004).
73 Precipitation and temperature in particular are often bias-corrected before they are used as
74 input to hydrologic models. Few studies explicitly discuss streamflow bias-correction (step 4
75 in figure 1). Hashino et al. (2007) evaluated three bias-correction methods (multiplicative
76 correction, regression method, and quantile mapping) to bias-correct ensemble streamflow
77 forecasts for a single site on the Des Moines River in Iowa, USA. Hamlet et al. (2013) used a
78 quantile mapping procedure to bias-correct streamflow estimates in a study of climate change
79 impacts on the hydrology of the Columbia River basin in the Pacific Northwest. Their bias-
80 correction procedure was based on earlier work by Snover et al. (2003) and Wood et al.
81 (2002) in which a monthly varying correction was calculated based on naturalized historical
82 flows and model simulations for the same period. These same corrections were then applied
83 to simulated flows under different climate scenarios. Farmer et al. (2018) used flow-duration-
84 curves to bias-correct simulated streamflow at ungauged locations. All these examples are
85 concerned with bias-correcting streamflow projections at longer timescales (generally greater
86 than a month, often over many years), which is the general type of application that we
87 considered during our method development as well. There may be other considerations in
88 bias-correcting short-term and real-time streamflow forecasts, which we will explore in the
89 discussion.

90 We focus on bias-correction methods for streamflow simulations and address two
91 shortcomings found in the existing methods as used in the previously discussed studies. First,
92 streamflow bias-correction methods that originate from the atmospheric science literature
93 tend to assume that bias-corrections can be applied independently at multiple locations on a
94 river network. In doing so, they ignore the upstream-downstream connection imposed by the
95 river network (which we refer to as spatial consistency). Bias-correction at upstream and
96 downstream sites treat the same parcels of water, that originated at the headwaters, in
97 potentially different ways. This alters the relationships between streamflow at upstream and
98 downstream sites and reduces the spatial-consistency of streamflow across a river network.
99 As a result, incremental flows between sites along a river network, which are often used as
100 input to water management models often become physically unrealistic, especially at shorter

101 time intervals (e.g. daily flows). For example, in the Missouri Headwaters Basin Study
102 (Bureau of Reclamation and Montana Department of Natural Resources and Conservation
103 2021), bias-corrected streamflow used as input to a water resources model was problematic,
104 because bias-corrections were developed independently for more than 20 sites, many of
105 which had overlapping watershed areas. The methods we propose in this paper address this
106 problem directly. An unrelated problem, which we do not address, was that reference
107 streamflow time series were based on multiple unrelated sources, which is often the case in
108 studies encompassing large watersheds. In the absence of a robust alternative methodology,
109 such as that described here, an ad hoc approach was developed to complete the Missouri
110 Headwaters Basin Study.

111 Second, many existing streamflow bias-correction methods assume stationarity in the
112 underlying processes between the reference period, which is used to train the bias-correction
113 method, and the application period, for example the end of the 21st century. This has been
114 shown to be a particularly important problem in the context of climate change projections
115 (Maraun 2016). Although some methods condition the bias-correction on time-of-year (for
116 example, a different quantile mapping for each month), the underlying assumption is that the
117 same quantile mapping is valid for the same time-of-year in the future. This can be
118 problematic. For example, imagine that a hydrologic model performs poorly in simulating
119 snow melt and that snow melt historically occurs during April. A monthly varying bias-
120 correction procedure would then indicate a large correction in April. However, under a
121 warming climate, snow melt may occur earlier or seasonal snow may disappear altogether
122 (Musselman et al. 2017; Livneh and Badger 2020). In this case, the bias-correction would
123 still result in a large bias-correction in April. This is because, as pointed out by Vrac and
124 Friederichs (2015), many bias-correction techniques are not able to change the timing (that is,
125 for example the “rank-chronology” as determined by the Spearman correlation) of the
126 corrected timeseries. While some multivariate bias-correction techniques do not strictly
127 adhere to this limitation (François et al. 2020; Cannon 2018; Clark et al. 2004), shifts in
128 timing are more of an indirect-effect rather than the primary purpose of the techniques, so
129 they are not suitable for correcting streamflow predictions in a changing climate. These
130 multivariate techniques which allow for shifts in timing usually aim to maintain or correct the
131 covariance structure between locations. However, for bias-correcting streamflow this is not
132 applicable because of the directional and tree-like structure of the river network topology.
133 Correcting for covariance structures on a river network would allow corrections at

134 downstream sites to “propagate” up the river network, which we generally consider
135 unphysical behavior. Similarly, models may have different biases under more extreme
136 conditions which may become more prevalent in the future climate (Slater et al. 2021),
137 thereby altering the cumulative distribution functions (CDFs) of simulated streamflow used
138 to calculate corrections. Rather than assuming stationarity for the underlying CDFs, we
139 would like to allow for non-stationarity in processes that are primarily responsible for the
140 systematic biases (process-conditioning).

141 We propose to preserve spatial consistency across the river network by bias-correcting
142 only the independent portions of the flows, that is, we correct the local flow contribution
143 from each individual sub-basin. Then, these locally bias-corrected flows can be re-aggregated
144 by a routing model that integrates surface runoff and upstream flow, as is normally done to
145 produce the total streamflow. Bias-correction of intervening flows automatically ensures
146 spatial consistency of the flows between upstream and downstream sites. This approach
147 requires estimation of local inflows at all locations, including sites for which we do not have
148 reference flows (for example, streamflow measurements).

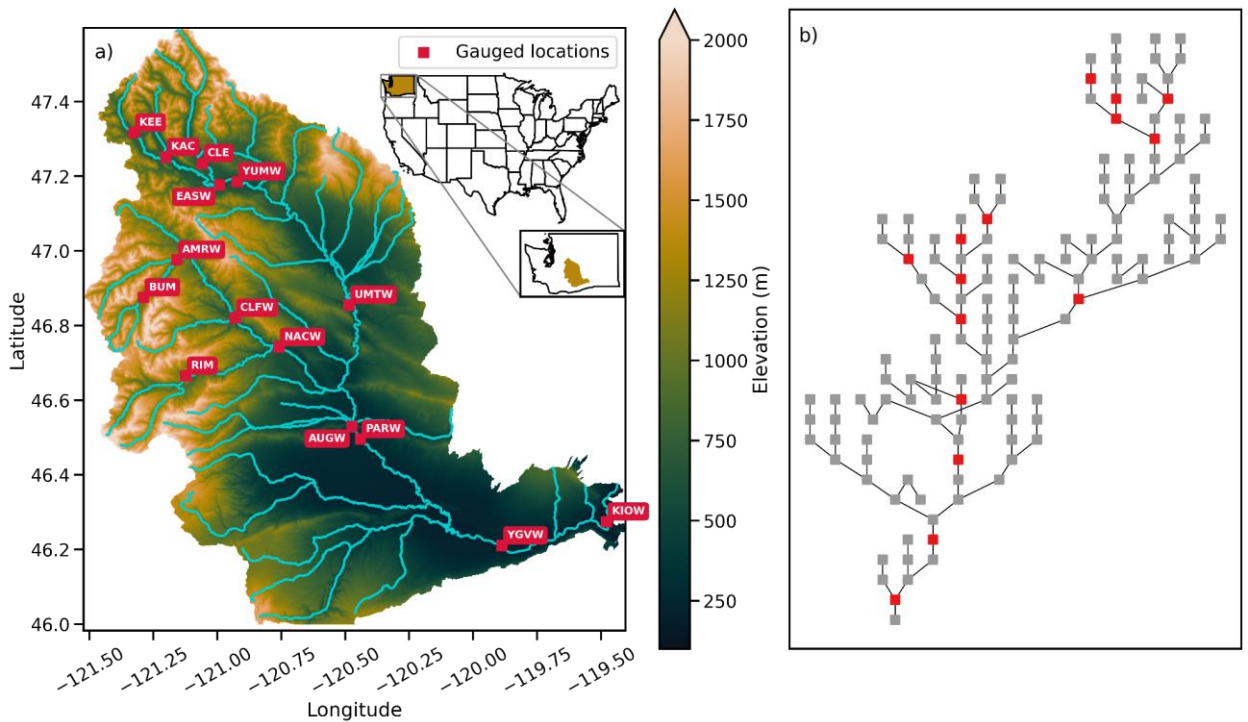
149 To allow for non-stationarity in the bias-correction and to allow for process-conditioning,
150 we propose to condition our bias-corrections with respect to another variable on which the
151 simulated errors may depend. This idea was originally proposed by Bellprat et al. (2013) who
152 suggested such a method might be useful for accounting for the role of soil moisture in the
153 correction of air temperatures. However, to our knowledge the idea remains untested for
154 streamflow bias-correction.

155 We evaluate our implementation of these bias-correction techniques on the Yakima River
156 Basin in the Pacific Northwestern United States and demonstrate their ability to better
157 preserve spatial consistency by comparing them against an independent bias-correction
158 technique. Further, we show how process-conditioning, while accounting for environmental
159 factors such as the air temperature, can improve bias-corrections. In section 2 we describe our
160 methodology, including both a description of the spatially-consistent bias-correction method
161 as well as our method of incorporating process-awareness into bias-correction methods. We
162 also outline details of the Yakima River Basin and data sources in section 2. In section 3 we
163 present the results of each of our test cases. Following the results, we discuss the current state
164 of our workflows and discuss future avenues for development in section 4. Finally, we
165 summarize and provide concluding remarks in section 5.

166 **2. Methods**

167 *a. Study region and data*

168 We apply our bias-correction techniques to the Yakima River Basin in the Pacific
169 Northwestern United States (figure 2). The Yakima River Basin is a 16 thousand square
170 kilometer sub-basin of the Columbia River Basin located on the eastern slopes of the Cascade
171 mountains in central Washington state. The Yakima River Basin has a strong gradient in
172 hydroclimate from the headwaters to the outlet. The headwaters are characterized by the
173 humid eastern slopes of the Cascade mountains and receive over 2500 mm of precipitation in
174 an average year. The outlet at the confluence of the Yakima and Columbia Rivers is arid,
175 receiving on average less than 250 mm of precipitation per year. This gradient in
176 precipitation coincides with a large gradient in elevation, with the headwaters exceeding an
177 elevation of 2000 meters and the outlet at just over 120 meters above mean sea level. Due to
178 orographic effects in the headwaters, most of the precipitation falls as snow through the fall
179 and winter months which drives a strong seasonal cycle in streamflow.



180

181 Figure 2. Yakima River Basin map. Gauged sites are shown in red, and are labeled with
182 their stream gauge abbreviations in panel a. The stream network topology, with gauged
183 locations highlighted in red is shown in panel b.

184

185 For this study we used simulations covering the entire Columbia river basin as described
 186 by Chegwiddden et al. (2019). In particular we use the runoff generated by the simulations at a
 187 daily timestep for the historical period covering water years 1980-2009, from the Variable
 188 Infiltration Capacity (VIC; Liang et al. 1994) model with the VIC-P1 parameter set
 189 (Chegwiddden et al. 2019). The resulting runoff fields from the VIC simulations were
 190 arranged on a 1/16° latitude-longitude grid, however the approach we take for streamflow
 191 routing is based on a vector, or unstructured, river network mesh. To align the simulated
 192 runoff to the river network we then remapped the gridded 1/16° VIC output onto the
 193 Geospatial Fabric unstructured mesh (Viger and Bock 2014) using a weighted averaging
 194 scheme. The remapped runoff is then routed through the river network using the mizuRoute
 195 river routing model (Mizukami et al. 2016) to produce the raw simulated streamflow that is
 196 analyzed in this study. We used the impulse response function routing method from
 197 mizuRoute in this implementation, though in principle the kinematic wave tracking routing
 198 method should also work. Our bias-correction technique can be run on either gridded or
 199 unstructured domains, and we chose to use the unstructured domain because we had the
 200 mizuRoute setup for the Yakima River available on the unstructured mesh.

201 Because neither VIC nor mizuRoute incorporates any land use or reservoir regulation
 202 components we use no regulation, no irrigation (NRNI) flows as our reference dataset instead
 203 of observations, which include the effects of human infrastructure (Pytlak et al. 2018). These
 204 NRNI flows were developed by the United States Army Corps of Engineers and the United
 205 States Bureau of Reclamation to produce flow estimates that are free of regulation and
 206 corrected for water withdrawals for irrigation. We used the NRNI flows to calculate the
 207 CDFs which are used to bias-correct the simulated flows. For all bias-corrections we use
 208 water years 1980-1991 to train the CDFs and 1992-2009 to apply the bias-corrections. Bias-
 209 correction is performed at the daily timestep.

210

Site	Winter Average Daily Low Temp (°C)	Summer Average Daily High Temp (°C)	Winter Average Precipitation (mm/day)	Summer Average Precipitation (mm/day)	Upstream Area (km ²)
KEE	-5.7	17.8	11.0	2.1	144

KAC	-4.6	21.1	7.1	0.9	167
EASW	-6.5	20.5	6.8	1.0	679
CLE	-5.3	22.8	4.6	0.5	526
YUMW	-6.5	23.3	4.7	0.7	1304
BUM	-8.2	17.9	6.8	0.9	192
AMRW	-8.2	17.5	6.9	1.0	206
CLFW	-8.3	21.3	5.3	0.8	1228
RIM	-6.5	22.0	4.2	0.6	485
NACW	-7.7	25.2	2.2	0.4	2437
UMTW	-6.9	26.3	1.7	0.4	4135
AUGW	-5.5	28.5	1.4	0.4	525
PARW	-4.3	29.7	0.9	0.3	9592
YGVW	-3.2	30.0	0.8	0.3	13767
KIOW	-3.1	29.6	1.0	0.3	14444

211 Table 1. Average meteorologic conditions at gauged sites which have reference NRNI
212 streamflow

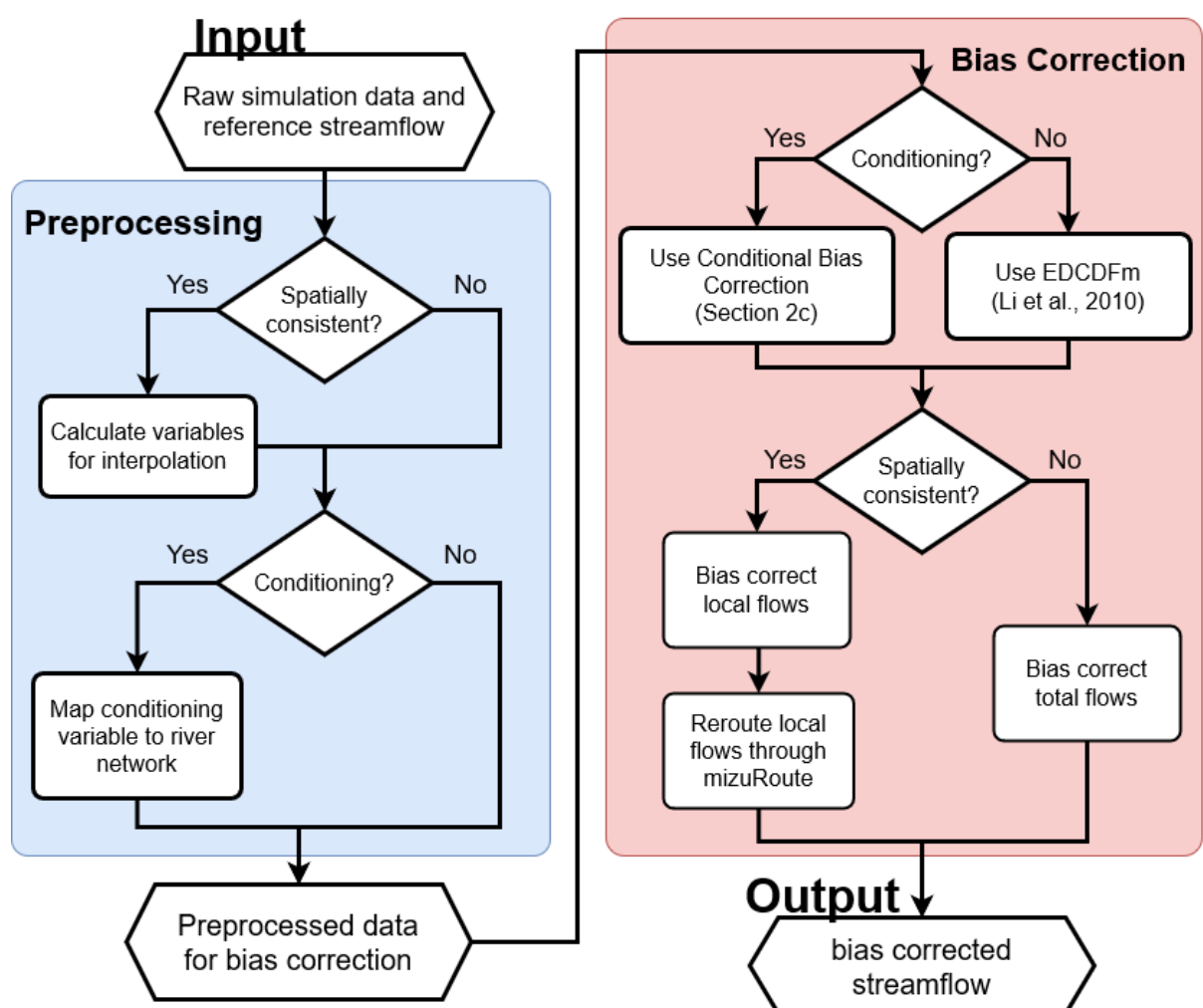
213

214 *b. Description of the bias-correction workflows*

215 The overall workflow for the bias-correction methods is shown in schematic form in
216 figure 3. The workflow is split into two pieces, a preprocessing step and the bias-correction
217 step. We built a reference implementation of this workflow in the software package, bmorph,
218 which is freely available and open source (Bennett et al. 2021). For specifics of the input data
219 requirements and configuration options see the bmorph documentation
220 (<https://bmorph.readthedocs.io>).

221 The preprocessing step depends on whether the chosen bias-correction method should
222 enforce spatial consistency and whether the chosen bias-correction method should consider
223 external variables through conditioning. If a spatially consistent method is selected the
224 locations of the reference gauges must be mapped onto the river network topology, which is

225 then used to locate upstream and downstream gauges for each river reach, along with an
 226 interpolation factor which is used to provide regionalized bias-corrections at each river reach.
 227 If process conditioning on another variable is used the other variable must also be associated
 228 with the underlying river network and gauge sites. For example, the meteorological data used
 229 to force the hydrologic model may not be on the same spatial domain as the river routing
 230 model, and so a way of selecting the meteorologic data which is overlapping with each river
 231 reach is determined in this step. We expand on the implementation of these bias-correction
 232 options in sections 2b and 2c, respectively. If neither of these options are selected, as in most
 233 traditional streamflow bias-correction methods, the preprocessing step may be omitted.



234
 235 Figure 3. Schematic of the workflow for the bias-correction options implemented in this
 236 study.

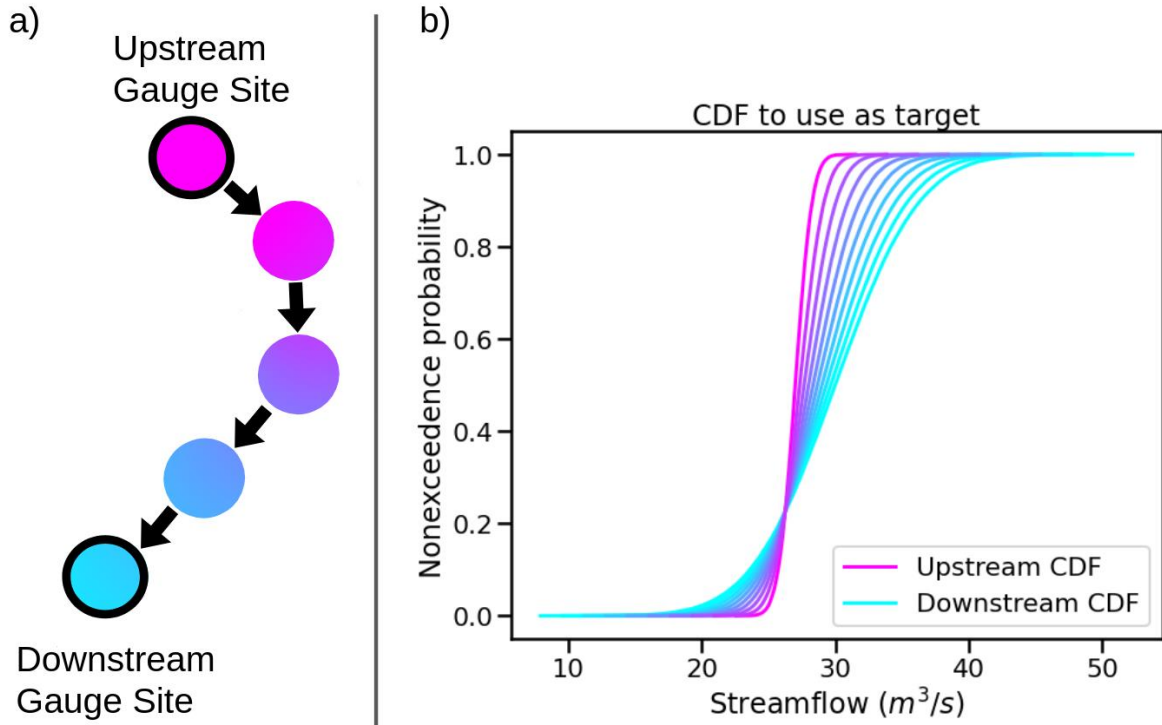
237
 238 Once preprocessing is complete, the resulting data can be input into the bias-correction
 239 workflow. This workflow also has branches for performing spatially consistent bias-
 240 correction and conditional bias-correction. The current implementation allows for these

241 options to be chosen independently, resulting in a flexible workflow that can be extended to
242 add additional steps and/or options. For instance, we provide two underlying bias-correction
243 techniques, the conditional bias-correction that we describe in section 2c and the Equidistant
244 Cumulative Distribution Function method (EDCDFm; Li et al. 2010). In principle any
245 number of other bias-correction techniques could be implemented independently of whether
246 spatially consistent bias-correction is used.

247 A post-processing technique similar to the one described in the PresRat method (Pierce et
248 al. 2015) was used to preserve changes in the mean flow between the training period and the
249 application period. Ours differs only in that it uses a rolling window (overlapping periods) of
250 365 days rather than a strided window (non-overlapping periods). For clarity, because two
251 methods of bias-correction were introduced in Pierce et al. (2015), the bias-correction
252 technique that we mimic for our underlying implementation is applied in the time domain
253 rather than the frequency domain.

254 *c. Spatially consistent bias-correction*

255 To implement a spatially consistent bias-correction technique for distributed streamflow
256 predictions we have developed a regionalization technique which interpolates the target
257 distribution between reference flow sites. A regionalization technique is required to perform
258 bias-corrections for each local inflow, many of which do not have associated reference flows.
259 The regionalization technique makes use of the topology of the river network by selecting
260 target distributions which are nearby and interpolating between them as a function of some
261 statistical measure (such as the correlation or a mean bias error). A schematic representation
262 of this interpolation is shown in figure 4.



263

264 Figure 4. Schematic of interpolated bias-correction. Panel a shows a schematic of stream
 265 segments where upstream and downstream gauge sites are highlighted with a black outline.
 266 Intermediate stream segments are colored via a linear color gradient. Panel b shows how
 267 CDFs are interpolated along the stream network. The color gradient of the CDFs matches the
 268 interpolation as you go from the upstream gauge site to the downstream gauge site in panel a.

269

270 When interpolating between gauged sites we use the formula:

$$271 \quad \tilde{Q}_{interp} = \alpha \cdot BC^{up}(Q_{oc}^{up}, Q_{mc}^{up}, Q_{mp}) + (1 - \alpha) \cdot BC^{down}(Q_{oc}^{down}, Q_{mc}^{down}, Q_{mp}) \quad (1)$$

272 where \tilde{Q}_{interp} is the bias-corrected streamflow for locations for which no reference flows
 273 are available, BC^i is the bias-correction function at either the upstream ($i = up$) or
 274 downstream ($i = down$) location, Q_{oc} is the observed or reference data, Q_{mc} represents the
 275 simulated streamflow values during the reference period, and Q_{mp} the simulated streamflow
 276 that will be bias-corrected. The values for α are computed in the preprocessing step, which is
 277 also when the locations of the upstream and downstream gauge sites for each river reach are
 278 recorded (figure 4).

279 The calculation of the α value can be done in a number of ways. For this study, we use
 280 the coefficient of determination (r^2) between the streamflow at each intermediate site and the
 281 up/downstream simulated streamflow to determine the interpolation factor. Given an

282 upstream streamflow, Q^{up} , and downstream streamflow, Q^{down} , then the interpolation factor
 283 for an intermediate streamflow, Q^i , is given by:

$$284 \quad \alpha = \frac{r^2(Q^i, Q^{up})}{r^2(Q^i, Q^{up}) + r^2(Q^i, Q^{down})} \quad (2)$$

285 Two edge cases for computing the interpolation factor require special handling. When
 286 there are no gauge sites to select either up or down stream, we use gauges at other locations
 287 in the network that have the highest r^2 value. When a site has multiple upstream gauge sites
 288 as tributaries, we similarly choose the site which has the highest r^2 value of the available
 289 upstream sites. While we use the coefficient of determination as our method of interpolating
 290 between sites, it is possible to implement this approach for a wide array of appropriate
 291 measures of similarity. Our reference implementation in `bmorph` also includes options to
 292 regionalize based on spatial distance, Kullback-Leibler divergence (Cover and Thomas
 293 2006), and Kling-Gupta efficiency (Gupta et al. 2009), though we have not explored how
 294 these choices affect the resulting bias-corrections.

295 To compute the bias-corrected local flows we take the ratio of the bias-corrected total
 296 flow and raw total flow, which results in a multiplier describing the relative change that
 297 should be applied to the local inflows. Given that Q^i is a total uncorrected streamflow, \tilde{Q}^i is
 298 the bias-corrected total streamflow from equation 1, and q^i is a local simulated streamflow,
 299 then we compute the bias-corrected local flow at each river reach as

$$300 \quad \tilde{q}^i = q^i \cdot \frac{\tilde{Q}^i}{Q^i} \quad (3)$$

301 These corrected local flows are then re-routed through `mizuRoute` to produce a spatially-
 302 consistent bias-corrected streamflow (SCBC).

303 *d. Conditional bias-correction*

304 We incorporate process information into the bias-correction scheme by modifying the
 305 EDCDFm algorithm (Li et al. 2010). The original EDCDFm equation is given as:

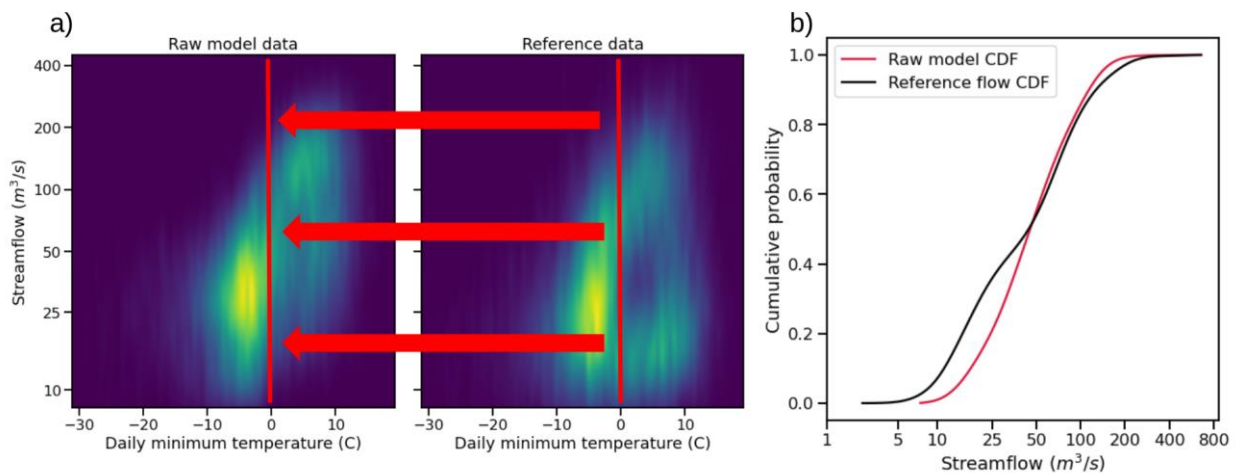
$$306 \quad \tilde{Q}_{mp} = Q_{mp} + F_{oc}^{-1} \left(F_{mp}(Q_{mp}) \right) - F_{mc}^{-1} \left(F_{mp}(Q_{mp}) \right) \quad (4)$$

307 where Q_{mp} is the modeled streamflow, F_{oc}^{-1} is the inverse of the CDF of the observed or
 308 reference data, F_{mp} is the CDF of the modeled projection, F_{mc} is the CDF of the modeled data

309 during the reference period, and \tilde{Q}_{mp} is the corrected modeled projection. This formulation is
 310 extended to condition on a two-dimensional (2-D) probability distribution function (PDF):

$$311 \quad \tilde{Q}_{mp} = Q_{mp} + F_{oc}^{-1}(F_{mp}(Q_{mp}|y_{mp})|y_{oc}) - F_{mc}^{-1}(F_{mp}(Q_{mp}|y_{mp})y_{mc}) \quad (5)$$

312 where y_i is the conditioning variable. To compute \tilde{Q}_{mp} we first calculate the 2-D PDF via
 313 a histogram estimator and then for each timestep at which we wish to correct, we compute the
 314 CDF conditioned on the value of y_i for that timestep (figure 5). We refer to this method as
 315 conditional bias-correction (CBC).



316

317 Figure 5. Schematic of conditional bias-correction (CBC). Panel a shows how
 318 conditioning on two-dimensional PDFs is computed. First, the PDFs are estimated from the
 319 data using histograms. In this example, we show the daily minimum temperature on the x-
 320 axis and streamflow on the y-axis. The left sub-plot shows the calculated PDF for the raw
 321 model data, while the right sub-plot shows the reference data. Areas of high probability are
 322 shown in brighter colors. The line at 0 °C indicates the position of conditioning for the daily
 323 minimum temperature. Panel b shows the CDF functions for both the raw and reference data
 324 as conditioned at 0 °C.

325

326 For this study we use as y_i the daily minimum temperature given by the forcing data
 327 which was used to run the VIC model and set the number of bins in our histogram estimator
 328 to be 100 in both dimensions, though these parameters are adjustable by the user. We use the
 329 daily minimum temperature because we hypothesize that there are snowmelt related biases in
 330 the late-spring and early-summer periods, as will be explored in the results.

331 *e. Evaluation Scenarios*

332 To evaluate the spatially consistent and conditional bias-correction methods in the
 333 Yakima River Basin, we compare the results of each of the combinations of the two new

334 methods against EDCDFm (Li et al. 2010). The four evaluation scenarios are detailed in
 335 Table 2. We refer to methods which use the blending as spatially consistent bias-correction
 336 (SCBC) techniques, while those that do not as independent bias-correction (IBC) techniques.
 337 Similarly, we denote methods which use the conditional bias-correction with C and those
 338 which do not condition as U (for univariate). In this case we refer to EDCDFm as IBC_U. By
 339 comparing each of the methods both independently and in conjunction we are better able to
 340 understand their impacts on bias-correction of streamflow.

	Spatially consistent BC (using interpolation)	Independent BC (no interpolation)
Univariate BC	SCBC_U	IBC_U
Conditional BC	SCBC_C	IBC_C

341 Table 2. Combinations of methods used in the analysis. Both the blending and
 342 conditioning can be turned on and off independently, leading to four bias-correction methods.

343

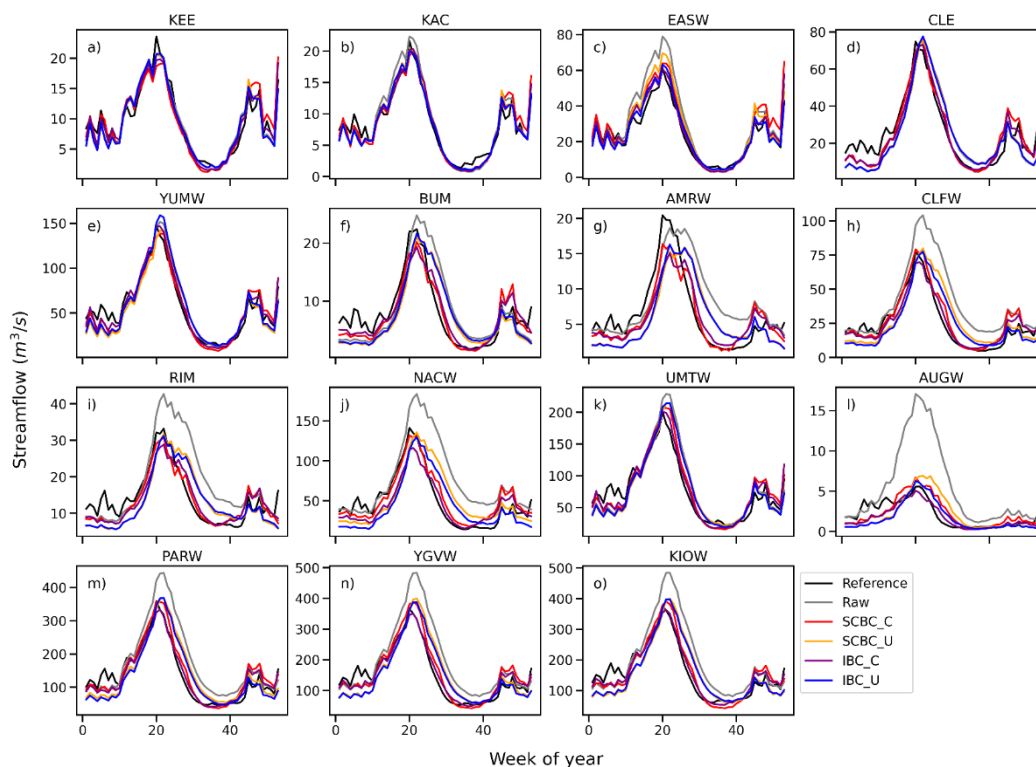
344 **3. Results**

345 Our results are organized into three sections which evaluate different aspects of the bias-
 346 correction process. In section 3a, we provide a general evaluation that compares the
 347 performance of the bias-correction methods across the Yakima River Basin. We show that all
 348 four correction methods can largely reduce the bias of the raw simulated streamflow, though
 349 some of their qualitative behaviors differ. In sections 3b and 3c, we further analyze these
 350 differences with respect to our two new methods. In section 3b, we show how conditioning
 351 on daily minimum temperatures improves the seasonal cycle of the bias-corrected streamflow
 352 as well as look at how the underlying probability distributions change with respect to the
 353 daily minimum temperature. In section 3c, we show how SCBC eliminates artifacts between
 354 river reaches. We also show how our SCBC method allows for finer grained analysis of bias-
 355 correction on spatially distributed streamflow simulations.

356 *a. General evaluation*

357 In figure 6, we show the mean weekly hydrographs for all scenarios (including raw and
 358 NRNI flows) for the bias-corrected period at each of the gauged sites. For the northern sub-

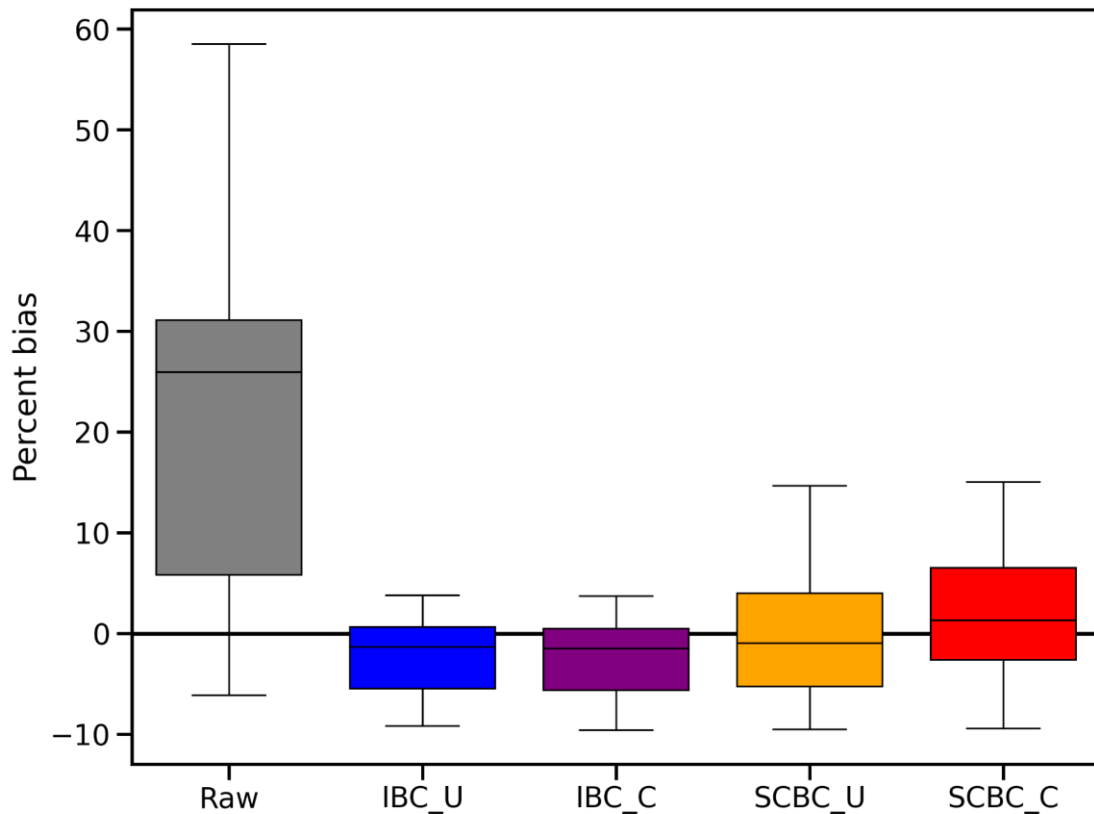
359 regions (KEE, KAC, EASW, CLE, YUMW, and BUM), we see general agreement between
 360 the raw flows and the NRNI flows. At some of the sites (notably CLE and BUM) we see
 361 improvements in timing with the conditional bias-correction methods. In the western portions
 362 of the catchment between UMTW and PARW (that is, at AMRW, CLFW, RIM, NACW, and
 363 AUGW) we see relative disagreement between methods. Generally, methods which were
 364 conditioned on daily minimum temperatures were better able to capture the falling limb of the
 365 summer streamflow, indicating resulting flows were corrected to better correspond with
 366 hydrologic processes associated with minimum temperature. At the downstream, mainstem
 367 sites (UMTW, YGVW, and KIOW) we see that the conditional bias-corrections were largely
 368 better at capturing the patterns of the NRNI streamflow.



369
 370 Figure 6. Mean weekly flows over the bias-corrected period for each of the scenarios
 371 arranged in approximate stream order (upper left as headwaters, lower right as outlet).

372
 373 Aggregating this into percent biases across both gauged sites and time (figure 7) we see
 374 that all methods are largely able to reduce the bias with respect to the raw simulations. The
 375 raw flows have a high bias of, on average, about 25%, while all other methods had biases of
 376 less than +/-5%. Additionally, the spread in the mean biases is reduced considerably for all
 377 bias-correction techniques. The IBC methods show about twice as much reduction in the

378 spread of biases as the SCBC methods, however the SCBC methods show better mean-bias
379 reductions.



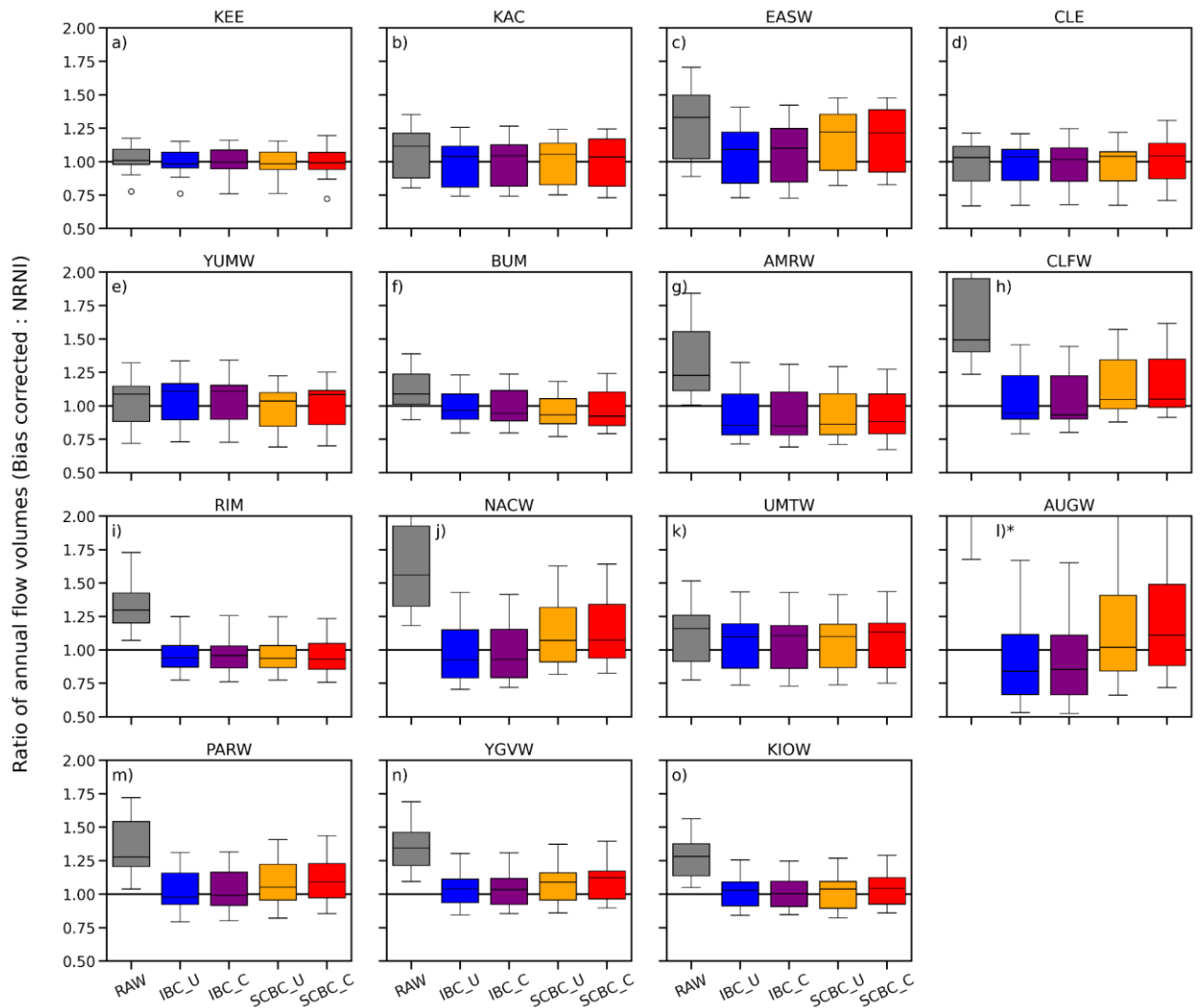
380

381 Figure 7. Boxplots of total percent biases across all sites and all time during the bias-
382 correction period. The center marker denotes the median percent bias, the ranges of the boxes
383 denote the interquartile range, and the whiskers extend to 1.5 times the interquartile range.
384 The ideal value of 0 is shown as a black line across the figure.

385

386 In addition to just the mean biases, water managers may also be interested in the annual
387 flow volumes throughout the river network. We analyze how these biases are changed at all
388 of the gauged sites for each bias-correction method in figure 8. Generally, we see that all of
389 the bias-correction methods improve the average and spread of the bias in annual flow
390 volumes. Differences between bias-correction methods are most apparent between IBC and
391 SCBC methods in the headwaters. At headwaters sites (e.g. EASW, BUM, and CLFW) we
392 generally see that IBC-based methods are better able to capture the annual flows, though
393 SCBC still provides better volumes than the uncorrected-predictions. We speculate that this is

394 because of the way we select the upstream reference flows in the headwaters, as discussed in
 395 section 2c. At the downstream locations (PARW, YGVW, and KLOW) we see that all bias-
 396 correction methods reduce the mean bias effectively, though the SCBC methods show higher
 397 variability in their ability to do so.



398

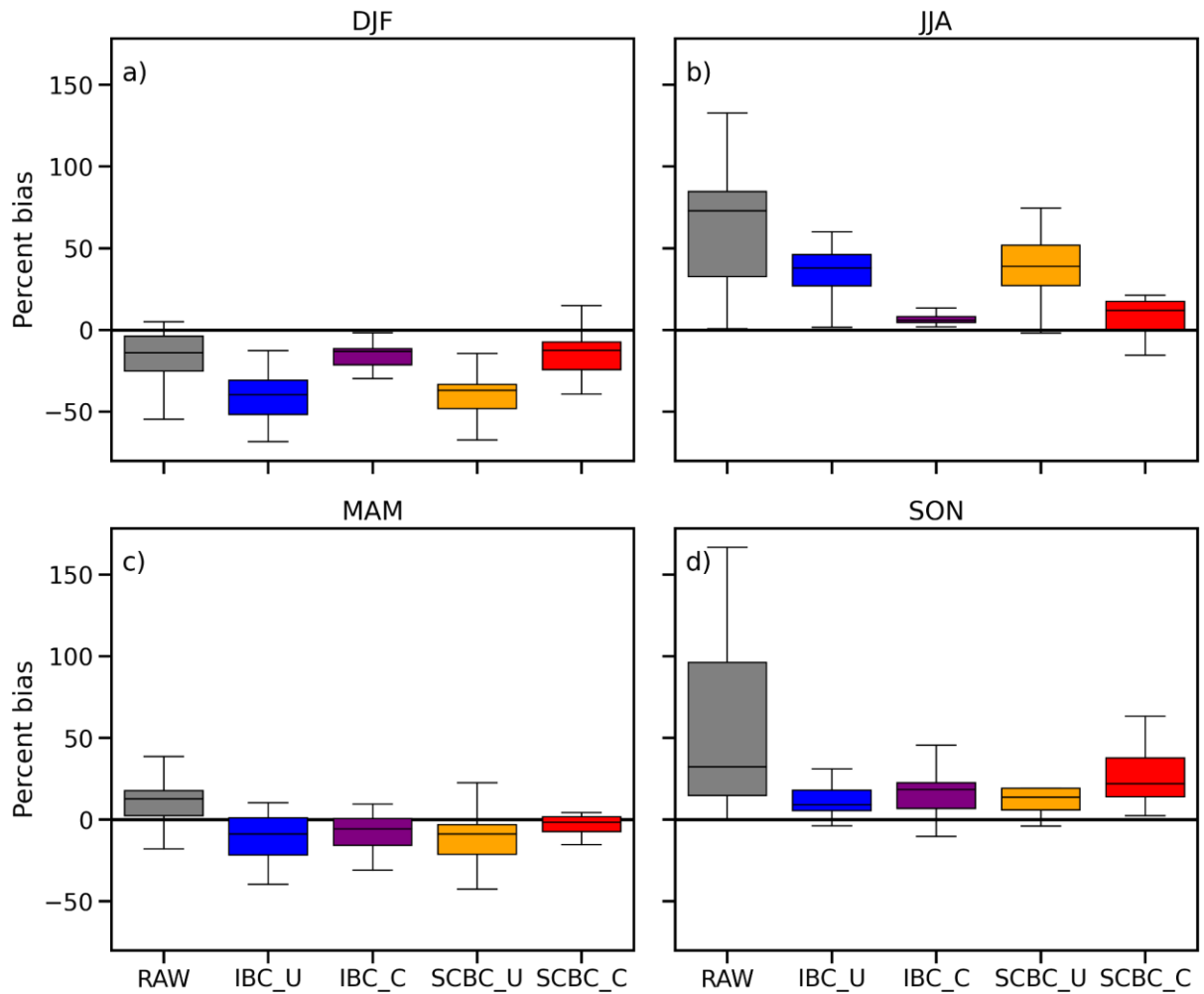
399 Figure 8. Boxplots of the ratio between each scenario and raw annual flow volumes
 400 during the application period (1992-2009, N=18). To calculate data for these boxplots we
 401 divided the cumulative annual streamflow for each method (RAW, IBC_U, etc) by the
 402 cumulative annual streamflow from the reference NRNI dataset for each water year. Subplot
 403 l) at AUGW is cut off to make the comparison across subplots easier. The center marker of
 404 each boxplot denotes the median percent bias, the ranges of the boxes denote the interquartile
 405 range, and the whiskers extend to 1.5 times the interquartile range. The ideal value of 1 is
 406 highlighted as a black horizontal line across each of the subplots.

407 *b. Effect of conditioning on the seasonal cycle*

408 To understand the effect of introducing a secondary variable to the bias-correction
 409 methodology. we analyzed the improvement of simulated streamflow for conditional bias-

410 correction methods (IBC_C and SCBC_C). From figure 6 we see that the conditioned bias-
411 correction methods are able to better match the timing of the falling limb of the hydrograph.
412 To quantify this effect, we calculate the percent biases on a seasonal basis, as shown in figure
413 9.

414 Generally, we see that for the winter and summer months (figure 9 panels a and b,
415 respectively) the conditioning on daily minimum temperature results in substantially reduced
416 bias from the raw flows. In the case of the winter season, the unconditioned bias-corrections
417 actually increased the flow biases. During the spring and fall seasons (figure 8 panels c and d,
418 respectively) we see that the conditioned bias-correction methods perform similarly to the
419 unconditioned variants. This is one indication that our choice in using the daily minimum
420 temperature as a proxy for model bias was a reasonable choice. We further explore this
421 choice in section 3c. While we could have chosen any number of other conditioning
422 variables, we chose daily minimum temperatures based on the knowledge of the underlying
423 hydrometeorology of the Yakima River Basin. In the discussion we expand on how we might
424 be able to more systematically understand or derive processes or variables to condition on.



425

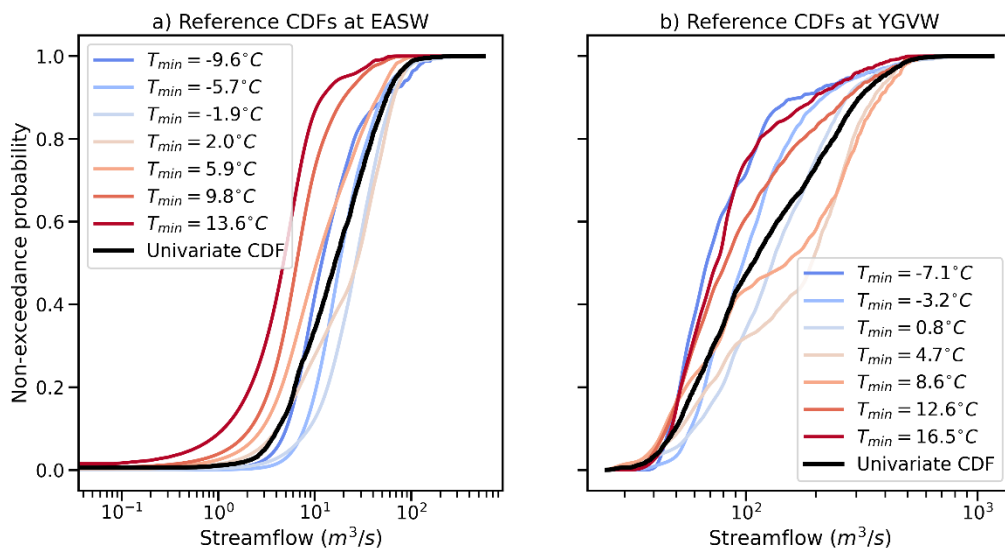
426 Figure 9. Boxplots of the percent bias for each of the seasons. Panel a shows the biases
 427 for all scenarios in winter months (DJF), panel b summer months (JJA), panel c spring
 428 months (MAM), and panel d fall months (SON). The center marker of each boxplot denotes
 429 the median percent bias, the ranges of the boxes denote the interquartile range, and the
 430 whiskers extend to 1.5 times the interquartile range. The ideal value of 0 is highlighted as a
 431 black horizontal line across each of the subplots.

432

433 To better understand how the conditioning on daily minimum temperature impacted bias-
 434 corrections we compute the reference CDFs across a range of values for the conditioning
 435 variable, daily minimum temperature, at basins in the headwaters (at EASW) and near the
 436 outlet along the mainstem (at YGVW) in figure 10. To do so, we first compute the joint 2-D
 437 PDFs and then marginalize on the values of T_{min} at equally spaced quantiles across the
 438 distribution of T_{min} . For both sites we found that there were substantial differences in the
 439 CDFs for different daily minimum temperatures. At EASW all of the CDFs appear to be

440 unimodal, though the steepness and location of the median flow changes with different
 441 temperatures.

442 However, at the downstream site (YGVW; figure 10 panel b), we see that the relative
 443 shapes of the CDFs change based on the daily minimum temperature. For both the low and
 444 high daily minimum temperatures the CDFs are generally steeper than the univariate
 445 equivalent and are still unimodal. However, the CDFs for the curves conditioned at $T_{min} =$
 446 $4.7\text{ }^{\circ}\text{C}$ and $T_{min} = 8.6\text{ }^{\circ}\text{C}$ have a bimodal structure. This is because the daily minimum
 447 temperature occurs in an annual cycle and that values corresponds to two different times of
 448 year with much different streamflow signatures, for example in spring temperatures are
 449 warming and in fall when temperatures are cooling. This is in contrast to the high and low
 450 values, which only occur in the summer and winter months, respectively. We further explore
 451 this choice of conditioning variable in the supplementary information and discuss the
 452 implications of using a conditioning variable with a seasonal cycle in section 4. Figure 10
 453 also gives us a way of anticipating how process-conditioned bias-correction methods will
 454 behave in a warming climate. In future conditions where we expect temperatures to be higher,
 455 this method would end up using more of the CDFs from the red lines and less from the blue
 456 lines.



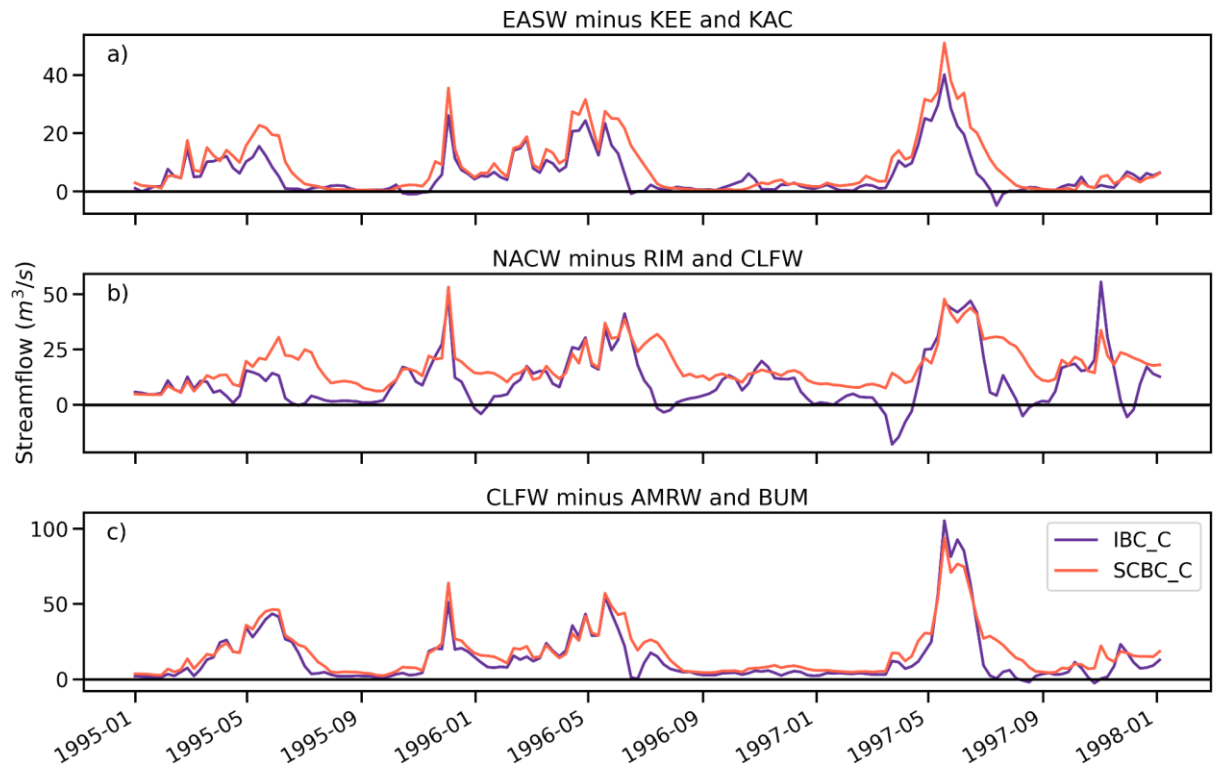
457

458 Figure 10. Comparison of cumulative distribution functions (CDFs) for univariate bias-
 459 correction (solid black line) and conditional bias-correction at several daily minimum
 460 temperatures (shaded blue to red lines). Panel a shows CDFs for a headwaters site (EASW)
 461 and panel b shows CDFs for a site on the mainstem of the Yakima River Basin near the outlet
 462 (YGVW).

463 *c. Effect of spatially consistent bias-correction*

464 Thus far we have only looked at the bias-corrections at each gauge location
465 independently, and though we have found that generally the SCBC-based methods are able to
466 reduce systematic bias in the simulated streamflow, they are not quite as performant as the
467 IBC methods. However, as discussed in the introduction, independently bias-corrected
468 streamflow can result in inconsistent behaviors for local inflows while the spatially consistent
469 method was designed to avoid these artifacts.

470 Figure 11 shows the weekly incremental streamflow at three locations (KEE, NACW, and
471 CLFW) on the Yakima River Basin. We determined the incremental streamflow (or local
472 inflow) by subtracting the flows at the upstream gauged sites. We chose to aggregate to the
473 weekly timescale to eliminate any artifacts of the transit time from upstream to downstream
474 gauged locations for IBC. In all three locations we found periods for which the IBC method
475 shows negative streamflow for at least a week, while SCBC maintains positive streamflow. It
476 is worth noting that in all three cases these are not losing reaches and that the negative
477 streamflow is purely an artifact of the bias-correction technique. This is most noticeable at
478 NACW with the inflows from RIM and CLFW removed, where these artificial negative
479 streamflow happen quite regularly and can be relatively large. While the resulting negative
480 flows are less at the other two sites shown in figure 11, they are an artifact of the method and
481 may cause errors in water management model simulations.

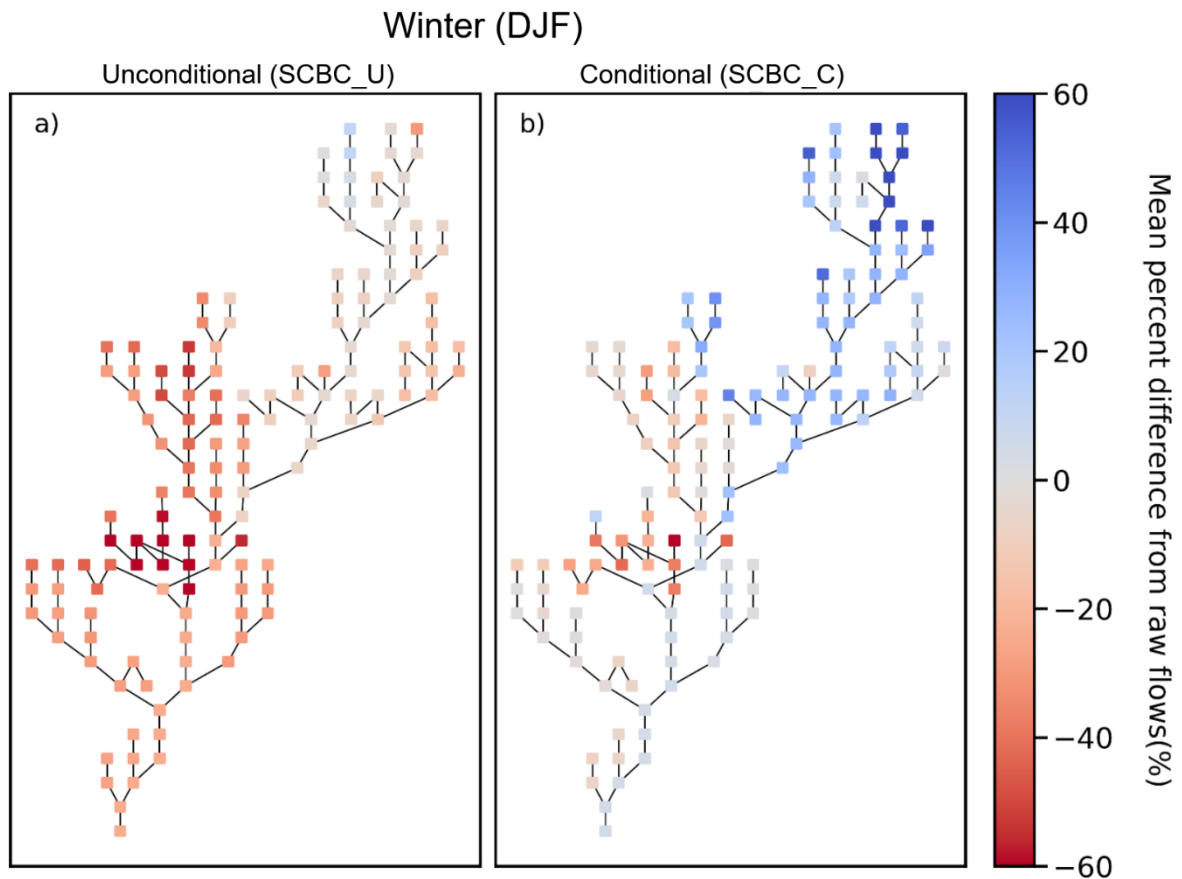


482

483 Figure 11. Comparison of streamflow with the streamflow from upstream gauged sites
 484 removed.

485

486 In addition to providing incremental streamflow at the gauged locations the SCBC
 487 method provides bias-corrected streamflow along every river reach in the simulation domain,
 488 something that the IBC methods do not provide. We show these as mean changes from the
 489 raw streamflow in figures 12 (winter streamflow) and 13 (summer streamflow). These figures
 490 show the spatial structure of the bias-corrections across the network. For both periods we see
 491 large, spatially coherent differences between unconditional corrections (SCBC_U) and
 492 conditional corrections (SCBC_C). During the winter period (figure 12) we see that
 493 unconditional bias-correction (SCBC_U) (figure 12a) largely works to decrease streamflow,
 494 except in the furthest headwaters. For conditional corrections (SCBC_C, figure 12b) we see
 495 that the bias-correction tended to increase streamflow, particularly along the upper portion of
 496 the basin. There are some decreases in the tributaries which flow into the mainstem further
 497 downstream, though not as drastic as the unconditional corrections (SCBC_U).

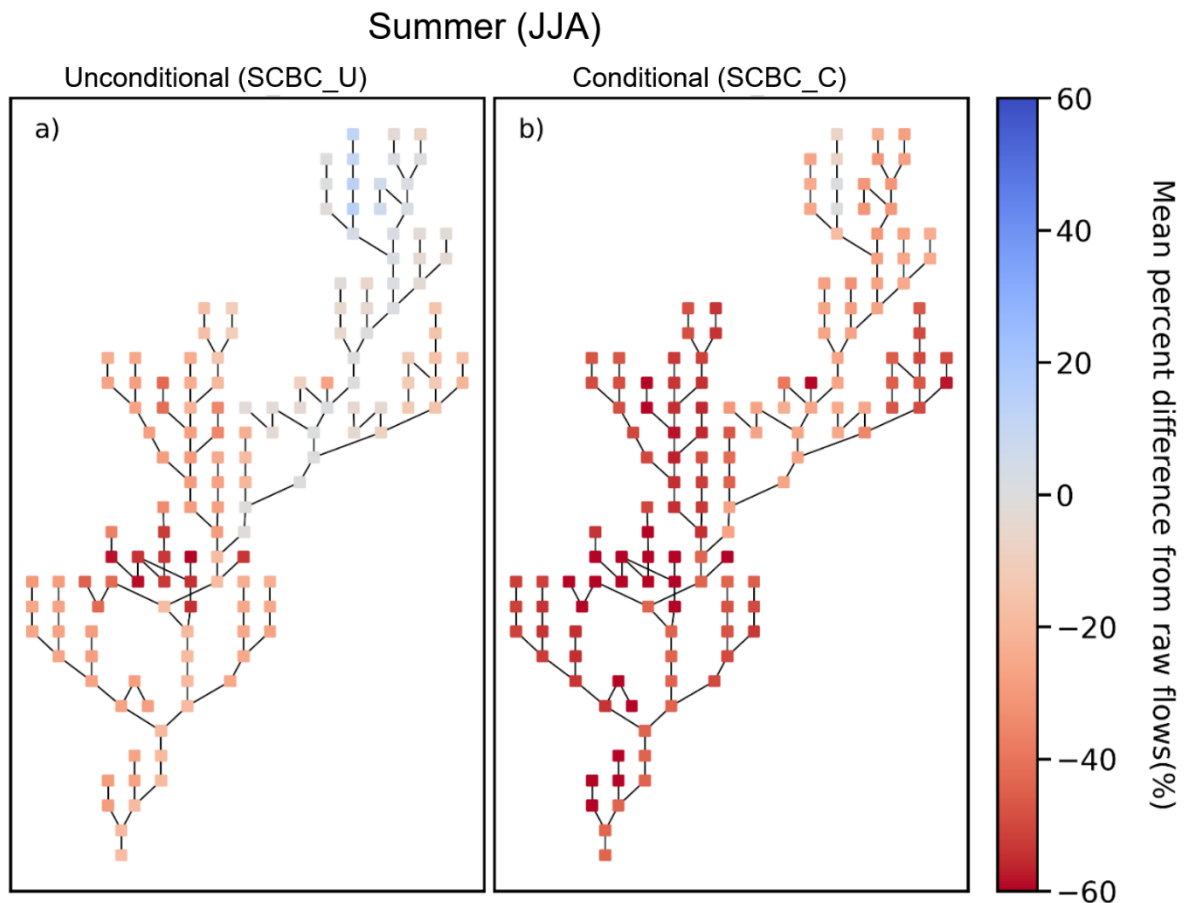


498

499 Figure 12. Change in the streamflow at each river reach in the Yakima River Basin for
 500 both spatially consistent configurations during winter (DJF).

501

502 The summer unconditional corrections (SCBC_U) (figure 13a) look similar to those in the
 503 winter (figure 12a), because the unconditional bias-correction is not able to modify the timing
 504 of the corrected streamflow. This can be seen in the annual corrections as well (figure S3, in
 505 the supplemental information). However, for conditional (SCBC_C) corrections in the
 506 summer (figure 13b) we see that there are drastic changes from the corrections of winter
 507 (figure 13b). During the summer SCBC_C almost universally decreases streamflow, with the
 508 exception of a few locations in the upper headwaters. The reduction in streamflow during the
 509 summer and increase in the winter from SCBC_C, particularly in the snowy headwaters,
 510 further demonstrates that conditionally bias-correcting on daily minimum temperatures can
 511 be a good proxy for errors in snow representation of the hydrologic model.



512

513 Figure 13. Change in the streamflow at each river reach in the Yakima River Basin for
 514 both spatially consistent configurations during summer (JJA).

515

516 4. Discussion

517 We have implemented and demonstrated two new techniques for bias-correcting
 518 distributed streamflow simulations. The first technique, spatially consistent bias-correction,
 519 allows for bias-correcting spatially distributed streamflow simulations explicitly, which
 520 maintains the relationships between gauged locations. The second technique, conditional
 521 bias-correction, allows for considering other variables during the bias-correction process by
 522 conditioning on a multidimensional probability distribution built on the streamflow as well as
 523 the other variables to be considered. We have shown that these methods can be developed in
 524 a modular and composable way (that is, we can arbitrarily choose to use spatially consistent
 525 methods and conditional methods independently) and have demonstrated their effects when
 526 applied separately as well as in conjunction.

527 The spatially consistent bias-correction method is built on a regionalization technique
528 which interpolates between gauged locations where reference streamflow is available. The
529 current implementation is based on interpolating between gauged locations based on the
530 correlation coefficient, though other methods of interpolation could, in principle, be
531 implemented in our framework. This method maintains spatial consistency by bias-correcting
532 the local flows at each stream segment, and then aggregating them through a river routing
533 model.

534 Our implementation of spatially consistent bias-correction in the Yakima River Basin
535 showed that correcting local streamflow directly and then rerouting it to recover the total
536 bias-corrected streamflow has similar performance in reducing bias as independent bias-
537 correction. Further, it produces bias-corrected streamflow at every river reach in the domain,
538 which can be used for other purposes, such as inputs into water management or other
539 operational models (Bureau of Reclamation and Montana Department of Natural Resources
540 and Conservation 2021). In addition to the benefits of producing bias-corrected local and total
541 streamflow at all river reaches, this approach eliminates artifacts in the relationship between
542 gauged locations that independent bias-correction can introduce.

543 The conditional bias-correction method is currently built by computing discretized PDFs
544 on streamflow and an additional conditioning variable via the histogram method. In this
545 study, we chose to use the daily minimum temperature as the conditioning variable, as a
546 proxy for snowmelt processes. We showed that conditioning on the daily minimum
547 temperature was able to improve the timing of the bias-corrected streamflow in the Yakima
548 River Basin. However, it remains an open question of how to choose the conditioning
549 variable in general. While it is theoretically possible to include more variables to condition
550 on, this becomes impractical quickly due to the curse of dimensionality, where the number of
551 possible variable combinations grows exponentially faster than the amount of data, ultimately
552 leading to empirically estimated PDFs which are very sparse, and thus noisy (Bellman 2010).
553 We anticipate that additional pre-bias-correction analysis will need to be done on a region-
554 by-region basis to determine which dominant processes to correct for.

555 In this study we were primarily interested in bias-correcting streamflow values over
556 multiple years. However, streamflow bias correction is also routinely applied over shorter
557 (hourly to monthly) timescales, for example as part of real-time forecasting operations..
558 While we have not evaluated the performance of our methods at these shorter timescales, we

559 note that quantile mapping based techniques are used in these applications as well. Because
560 of this, we hypothesize that the process-conditioned bias-correction technique could translate
561 well to shorter-scale applications, particularly by conditioning on the initial state of the
562 hydrologic model, which is often a large source of error in the forecasts. However, we
563 anticipate that modifications would be needed to ensure that these approaches could be
564 transferred without unanticipated consequences.

565 **5. Conclusions**

566 Our results from implementing two modular and composable streamflow bias-correction
567 techniques show how bias-correction techniques, which are designed with streamflow in
568 mind, can make improvements over existing methods. Our simple regionalization technique
569 based on interpolating between gauged locations provides spatially distributed (and spatially
570 consistent) bias-corrections, while still maintaining performance close to the performance of
571 bias-corrections that are tuned at each individual gauge location independently. We also show
572 that correcting on daily minimum temperatures via conditional bias-correction can improve
573 the timing of the bias-corrected streamflow over the unconditioned bias-corrections across
574 seasons in the Yakima River Basin. The choice of the specific conditioning variable in the
575 conditional bias correction method is flexible and can be based on locally dominant
576 processes.

577 Reducing bias in simulated streamflow is critical when it is used as input to a water
578 resources model for the purpose of evaluating scenarios for long-term water management and
579 planning. Federal agencies such as the Bureau of Reclamation rely on these techniques to
580 study how scenarios of future hydrology may impact existing reservoir operations, for
581 example. These studies may inform future investments in infrastructure or modifications to
582 operations. Refinement of bias-correction techniques may help reduce uncertainty in planning
583 scenarios, thereby saving costs in structural or non-structural modifications that may be based
584 on over-conservative planning to compensate for future uncertainty. Currently, water
585 managers rely on ad hoc approaches to developing local inflows based on streamflow
586 simulations and simply live with the concept that bias-correction techniques cannot address
587 changing streamflow timing. Alternative methods, such as the SCBC_C method described
588 here are critical steps toward reducing uncertainties in planning scenarios.

589 By demonstrating two approaches to bias-correcting streamflow simulations we find that
590 improvements can be made to the previously used methods that are generally taken from
591 bias-correcting climate and atmospheric models. By designing correction techniques which
592 target distributed streamflow simulations we can design new bias-correction methods which
593 perform well. However, these initial implementations were often built around the simplest
594 possible method. Improving the way which interpolation between gauged locations, handling
595 headwaters which flow into the mainstem, and allowing for conditioning on multiple
596 variables may improve these methods further.

597 The results of our bias-correction techniques are based on our initial workflow
598 implementation. We have developed a python package, *bmorph*, which includes the
599 implementation that was used for this analysis (Bennett et al. 2021). It also includes the setup
600 for the Yakima River Basin as analyzed here as a tutorial dataset. The code and data for
601 running this analysis is also available at [doi:10.5281/zenodo.5348461](https://doi.org/10.5281/zenodo.5348461). We have designed
602 *bmorph* in a way that allows it to be modular and extensible, making it easy to build on the
603 initial implementations that we have described here.

604 *Acknowledgments.*

605 This study was funded in part by the U.S. Bureau of Reclamation Science and
606 Technology program under project ID 1895. We thank Nathalie Voisin, Andy Wood, and
607 Naoki Mizukami for insightful comments and for help with *mizuRoute*.

608 *Data Availability Statement.*

609 The data and analysis for this study is available at doi.org/10.5281/zenodo.5348461. We
610 have released the *bmorph* package as a freely available and open-source python package at
611 doi.org/10.5281/zenodo.5348463.

612 REFERENCES

613 Bellman, R., 2010: *Dynamic Programming*. Princeton University Press, 392 pp.

614 Bellprat, O., S. Kotlarski, D. Lüthi, and C. Schär, 2013: Physical constraints for
615 temperature biases in climate models. *Geophys. Res. Lett.*, **40**, 4042–4047,
616 <https://doi.org/10.1002/grl.50737>.

617 Bennett, A., B. Nijssen, A. Stein, B. Lounsbury, and O. Chegwidden, 2021: UW-
618 Hydro/*bmorph*: v1.0.0. <https://doi.org/10.5281/zenodo.5348463>.

619 Bosshard, T., M. Carambia, K. Goergen, S. Kotlarski, P. Krahe, M. Zappa, and C. Schär,
620 2013: Quantifying uncertainty sources in an ensemble of hydrological climate-impact
621 projections. *Water Resour. Res.*, **49**, 1523–1536, <https://doi.org/10.1029/2011WR011533>.

622 Bureau of Reclamation, and Montana Department of Natural Resources and
623 Conservation, 2021: Missouri Headwaters Basin Study. 149.

624 Cannon, A. J., 2018: Multivariate quantile mapping bias correction: an N-dimensional
625 probability density function transform for climate model simulations of multiple variables.
626 *Clim. Dyn.*, **50**, 31–49, <https://doi.org/10.1007/s00382-017-3580-6>.

627 Chegwiddden, O. S., and Coauthors, 2019: How Do Modeling Decisions Affect the Spread
628 Among Hydrologic Climate Change Projections? Exploring a Large Ensemble of Simulations
629 Across a Diversity of Hydroclimates. *Earths Future*, **7**, 623–637,
630 <https://doi.org/10.1029/2018EF001047>.

631 Chen, J., F. P. Brissette, D. Chaumont, and M. Braun, 2013: Finding appropriate bias
632 correction methods in downscaling precipitation for hydrologic impact studies over North
633 America. *Water Resour. Res.*, **49**, 4187–4205, <https://doi.org/10.1002/wrcr.20331>.

634 Clark, M., S. Gangopadhyay, L. Hay, B. Rajagopalan, and R. Wilby, 2004: The Schaake
635 Shuffle: A Method for Reconstructing Space–Time Variability in Forecasted Precipitation
636 and Temperature Fields. *J. Hydrometeorol.*, **5**, 243–262, [https://doi.org/10.1175/1525-7541\(2004\)005<0243:TSSAMF>2.0.CO;2](https://doi.org/10.1175/1525-7541(2004)005<0243:TSSAMF>2.0.CO;2).

638 Cover, T. M., and J. A. Thomas, 2006: *Elements of Information Theory (Wiley Series in*
639 *Telecommunications and Signal Processing)*. Wiley-Interscience,.

640 Farmer, W. H., T. M. Over, and J. E. Kiang, 2018: Bias correction of simulated historical
641 daily streamflow at ungauged locations by using independently estimated flow duration
642 curves. *Hydrol. Earth Syst. Sci.*, **22**, 5741–5758, <https://doi.org/10.5194/hess-22-5741-2018>.

643 François, B., M. Vrac, A. J. Cannon, Y. Robin, and D. Allard, 2020: Multivariate bias
644 corrections of climate simulations: which benefits for which losses? *Earth Syst. Dyn.*, **11**,
645 537–562, <https://doi.org/10.5194/esd-11-537-2020>.

646 Guo, Q., J. Chen, X. J. Zhang, C.-Y. Xu, and H. Chen, 2020: Impacts of Using State-of-
647 the-Art Multivariate Bias Correction Methods on Hydrological Modeling Over North
648 America. *Water Resour. Res.*, **56**, e2019WR026659, <https://doi.org/10.1029/2019WR026659>.

649 Gupta, H. V., H. Kling, K. K. Yilmaz, and G. F. Martinez, 2009: Decomposition of the
650 mean squared error and NSE performance criteria: Implications for improving hydrological
651 modelling. *J. Hydrol.*, **377**, 80–91, <https://doi.org/10.1016/j.jhydrol.2009.08.003>.

652 Hamlet, A. F., M. M. Elsner, G. S. Mauger, S.-Y. Lee, I. Tohver, and R. A. Norheim,
653 2013: An Overview of the Columbia Basin Climate Change Scenarios Project: Approach,
654 Methods, and Summary of Key Results. *Atmosphere-Ocean*, **51**, 392–415,
655 <https://doi.org/10.1080/07055900.2013.819555>.

656 Hashino, T., A. A. Bradley, and S. S. Schwartz, 2007: Evaluation of bias-correction
657 methods for ensemble streamflow volume forecasts. *Hydrol Earth Syst Sci*, **12**.

658 Li, H., J. Sheffield, and E. F. Wood, 2010: Bias correction of monthly precipitation and
659 temperature fields from Intergovernmental Panel on Climate Change AR4 models using
660 equidistant quantile matching. *J. Geophys. Res. Atmospheres*, **115**,
661 <https://doi.org/10.1029/2009JD012882>.

662 Liang, X., D. P. Lettenmaier, E. F. Wood, and S. J. Burges, 1994: A simple
663 hydrologically based model of land surface water and energy fluxes for general circulation
664 models. *J. Geophys. Res. Atmospheres*, **99**, 14415–14428,
665 <https://doi.org/10.1029/94JD00483>.

666 Livneh, B., and A. M. Badger, 2020: Drought less predictable under declining future
667 snowpack. *Nat. Clim. Change*, **10**, 452–458, <https://doi.org/10.1038/s41558-020-0754-8>.

668 Maraun, D., 2013: Bias Correction, Quantile Mapping, and Downscaling: Revisiting the
669 Inflation Issue. *J. Clim.*, **26**, 2137–2143, <https://doi.org/10.1175/JCLI-D-12-00821.1>.

670 ———, 2016: Bias Correcting Climate Change Simulations - a Critical Review. *Curr. Clim.*
671 *Change Rep.*, **2**, 211–220, <https://doi.org/10.1007/s40641-016-0050-x>.

672 Mizukami, N., and Coauthors, 2016: mizuRoute version 1: a river network routing tool
673 for a continental domain water resources applications. *Geosci. Model Dev.*, **9**, 2223–2238,
674 <https://doi.org/10.5194/gmd-9-2223-2016>.

675 Musselman, K. N., M. P. Clark, C. Liu, K. Ikeda, and R. Rasmussen, 2017: Slower
676 snowmelt in a warmer world. *Nat. Clim. Change*, **7**, 214–219,
677 <https://doi.org/10.1038/nclimate3225>.

678 Pierce, D. W., D. R. Cayan, E. P. Maurer, J. T. Abatzoglou, and K. C. Hegewisch, 2015:
679 Improved Bias Correction Techniques for Hydrological Simulations of Climate Change. *J.*
680 *Hydrometeorol.*, **16**, 2421–2442, <https://doi.org/10.1175/JHM-D-14-0236.1>.

681 Pytlak, E., C. Frans, K. Duffy, J. Johnson, B. Nijssen, O. Chegwidan, and D. Rupp,
682 2018: *Climate and Hydrology Datasets for RMJOC Long-Term Planning Studies: Second*
683 *Edition*. <https://www.bpa.gov/p/Generation/Hydro/hydro/cc/RMJOC-II-Report-Part-I.pdf>
684 (Accessed August 24, 2021).

685 Shi, X., A. W. Wood, and D. P. Lettenmaier, 2008: How Essential is Hydrologic Model
686 Calibration to Seasonal Streamflow Forecasting? *J. Hydrometeorol.*, **9**, 1350–1363,
687 <https://doi.org/10.1175/2008JHM1001.1>.

688 Slater, L. J., and Coauthors, 2021: Nonstationary weather and water extremes: a review of
689 methods for their detection, attribution, and management. *Hydrol. Earth Syst. Sci.*, **25**, 3897–
690 3935, <https://doi.org/10.5194/hess-25-3897-2021>.

691 Snover, A. K., A. F. Hamlet, and D. P. Lettenmaier, 2003: Climate-Change Scenarios for
692 Water Planning Studies. 6.

693 Viger, R., and A. Bock, 2014: GIS Features of the Geospatial Fabric for National
694 Hydrologic Modeling. <https://doi.org/10.5066/F7542KMD>.

695 Vrac, M., and P. Friederichs, 2015: Multivariate—Intervariable, Spatial, and Temporal—
696 Bias Correction. *J. Clim.*, **28**, 218–237, <https://doi.org/10.1175/JCLI-D-14-00059.1>.

697 Wilby, R. L., and S. Dessai, 2010: Robust adaptation to climate change. *Weather*, **65**,
698 180–185, <https://doi.org/10.1002/wea.543>.

699 Wood, A. W., E. P. Maurer, A. Kumar, and D. P. Lettenmaier, 2002: Long-range
700 experimental hydrologic forecasting for the eastern United States. *J. Geophys. Res.*
701 *Atmospheres*, **107**, ACL 6-1-ACL 6-15, <https://doi.org/10.1029/2001JD000659>.

702 Wood, A. W., L. R. Leung, V. Sridhar, and D. P. Lettenmaier, 2004: Hydrologic
703 Implications of Dynamical and Statistical Approaches to Downscaling Climate Model
704 Outputs. *Clim. Change*, **62**, 189–216, <https://doi.org/10.1023/B:CLIM.0000013685.99609.9e>.

705